970 J. Med. Chem. 2011, 54, 970–979
DOI: 10.1021/jm101198k

Journal of Medicinal Chemistry Article

# *In Vivo* Trypanosomicidal Activity of Imidazole- or Pyrazole-Based Benzo[*g*]phthalazine Derivatives against Acute and Chronic Phases of Chagas Disease

Manuel Sánchez-Moreno,*[,§] Ana M. Sanz,[†] Fernando Gómez-Contreras,*[,†] Pilar Navarro,[‡] Clotilde Marín,[§] Inmaculada Ramírez-Macias,[§] María Jose Rosales,[§] Francisco Olmo,[§] Isabel Garcia-Aranda,[‡] Lucrecia Campayo,[†] Carmen Cano,[†] Francisco Arrebola,[¥] and María J. R. Yunta[†]

[§]*Instituto de Biotecnología, Facultad de Ciencias, Universidad de Granada, 18071 Granada, Spain,* [†]*Departamento de Química Orgánica, Facultad de Química, Universidad Complutense, E-28040 Madrid, Spain,* [‡]*Instituto de Química Médica, Centro de Química Orgánica M. Lora-Tamayo, CSIC, E-28006 Madrid, Spain, and* [¥]*Departamento de Histología, Facultad de Medicina, Universidad de Granada, Spain*

*Received September 15, 2010*

The *in vivo* trypanosomicidal activity of the imidazole-based benzo[*g*]phthalazine derivatives **1**−**4** and of the new related pyrazole-based compounds **5** and **6** has been studied in both the acute and chronic phases of Chagas disease. As a rule, compounds **1**−**6** were more active and less toxic than benznidazole in the two stages of the disease, and the monosubstituted derivatives **2**, **4**, and **6** were more effective than their disubstituted analogs. Feasible mechanisms of action of compounds **1**−**6** against the parasite have been explored by considering their inhibitory effect on the Fe-SOD enzyme, the nature of the excreted metabolites and the ultrastructural alterations produced. A complementary histopathological analysis has confirmed that the monosubstituted derivatives are less toxic than the reference drug, with the behavior of the imidazole-based compound **4** being especially noteworthy.

## Introduction

Tropical and subtropical diseases caused by protozoal parasites remain a major public health problem in many less developed countries, because of the lack of effective drugs or because of increasing resistance against the few affordable drugs.[1,2] American trypanosomiasis, also known as Chagas disease, is one of the most devastating. It is caused by the kinetoplastid protozoan *Trypanosoma cruzi*, which is vectorially transmitted by a bug depositing feces on and subsequently biting the skin surface. Other routes of contamination are infected blood transfusions, organ transplantation, and even mother-to-child transmission during pregnancy or breastfeeding.[3] Chagas disease takes the form of an acute infection, during which most patients do not know that they are infected, with further evolution to a chronic and systemic stage severely affecting the heart, esophagus, and colon. It is endemic throughout all Latin America and is classed by the WHO[a] as the third most widespread tropical disease after malaria and schistosomiasis.[4] It is estimated that about 100 million people are at risk of infection, that from 15 to 20 million people are infected, and that 50000 die annually as a result of infection by this parasite.

Unfortunately, current treatment for this disease is very limited, and no successful vaccine has been developed.[5] The drugs available are mainly nitroheterocyclic compounds like the nitrofurane nifurtimox or the nitroimidazole derivative benznidazole, but they are only effective against the acute phase, exhibiting very limited efficacy in the chronic stage.[6] Furthermore, they are quite toxic and cause severe side effects like pancreatitis and cardiac toxicity.[7] The search for more effective drugs is mainly centered on their potential action against essential and exclusive components of the trypanosomatids. Targets under study are 6-phosphogluconate dehydrogenase or dihydrofolate reductase, a key enzyme for DNA synthesis.[8] Another promising target is the iron superoxide dismutase (Fe-SOD). This enzyme is found exclusively in protozoa and plays an essential antioxidant role in the survival of the parasite, due to its scavenging ability for the superoxide anion.[9] The action against enzymes involved in the biosynthesis of trypanothione, which also represents an important defense barrier against oxidative damage, is being investigated.[10] This is the case with ornithine decarboxylase (ODC), *S*-adenosylmethionine decarboxylase (AdoMet-DC), spermidine synthase (SpdS), trypanothione synthase (TryS), and trypanothione reductase (TryR).

In close connection with this matter, our research group has been preparing heteroaromatic compounds containing the 1-alkylamino- or 1,4-bisalkylaminobenzo[*g*]-phthalazine system, which exhibit interesting transition metal-complexing properties and have shown remarkable *in vitro* antiparasitic activity[11] (Figure 1). We have described in a recent study that the introduction of imidazole units in the flexible side chains of the benzo[*g*]phthalazine system (Figure 2, compounds **1**−**4**)

*To whom correspondence should be addressed. Fernando Gomez-Contreras: Phone: +34-91-394-4229, fax: +34-91-394-4103, E-mail: fercon@quim.ucm.es. Manuel Sanchez-Moreno: Phone: +34-958-242-369, fax: +34-958-243-862, E-mail: msanchem@ugr.es.

[a] Abbreviations: SOD, superoxide dismutase; WHO, World Health Organization; ODC, ornithine decarboxylase; AdoMet-DC, adenosylmethionine decarboxylase; SpdS, spermidine synthase; TryS, trypanothione synthase; TryR, trypanothione reductase; BZN, benznidazole; TEM, transmission electron microscopy; HMQC, heteronuclear single quantum coherence experiment; HMBC, heteronuclear multiple bond coherence experiment; dpi, days postinfection; TLC, thin-layer chromatography; TMS, tetramethylsilane, MEM, minimal essential medium; NAD(P)H, nicotinamide adenine dinucleotide phosphate.

 Published on Web 01/13/2011 

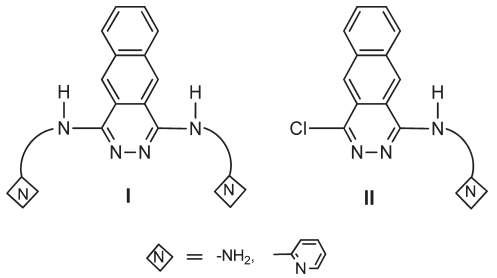

**Figure 1.** Models for the design of benzo[*g*]phthalazine derivatives with potential antiparasitic activity.

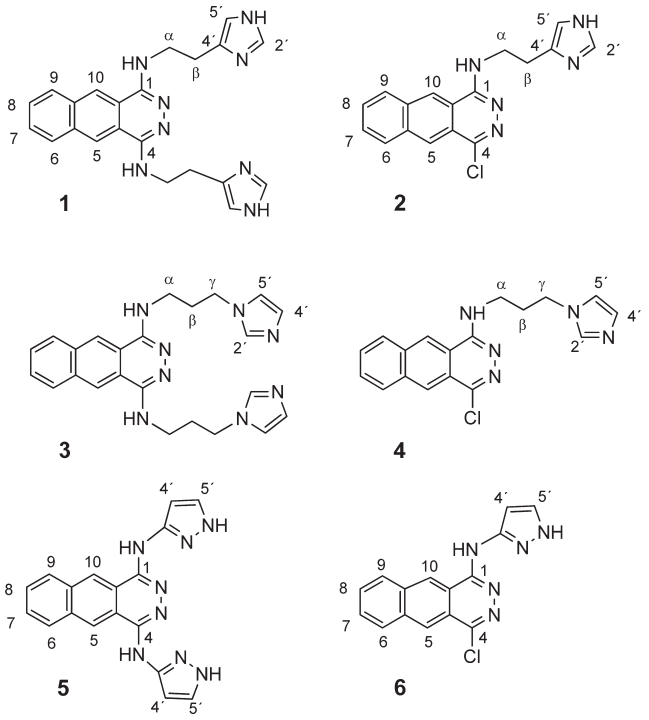

**Figure 2.** Imidazole- (**1**−**4**) and pyrazole-based (**5**,**6**) structures tested *in vivo* against *T. cruzi*.

enhances their *in vitro* trypanosomicidal activity against *T. cruzi* and also show the ability to inhibit the crucial antioxidant Fe-SOD enzyme.[12]

Even more interestingly, these compounds also exhibit very low *in vitro* toxicity against Vero cells with respect to a typical antiparasitic drug like benznidazole. Taking into account the considerable complexing ability toward metal ions shown by our compounds,[11] we think that competitive complexation for the metal ion of SOD could be an effective way of deactivating the antioxidant protective effect of the enzyme,[13] which will affect both the growth and survival of parasitic cells.

These results prompted us to design two new related compounds lacking the flexible methylene groups at the side chains, in which the imidazole units have been replaced by pyrazole rings (Figure 2, compounds **5** and **6**). Although pyrazoles are rarely found in nature, they are present in many pharmaceuticals with a wide range of biological activities.[14] Even more, pyrazoles are effective tools in supramolecular chemistry, and their conjugate bases have been found to bind metals in a variety of coordination modes and are considered robust bridging ligands.[15,16] The increased system rigidity and the presence of a heterocyclic ring with well-known complexing abilities could allow a cooperative action of both the

**Scheme 1.** Synthesis of the New Pyrazole-Based Derivatives

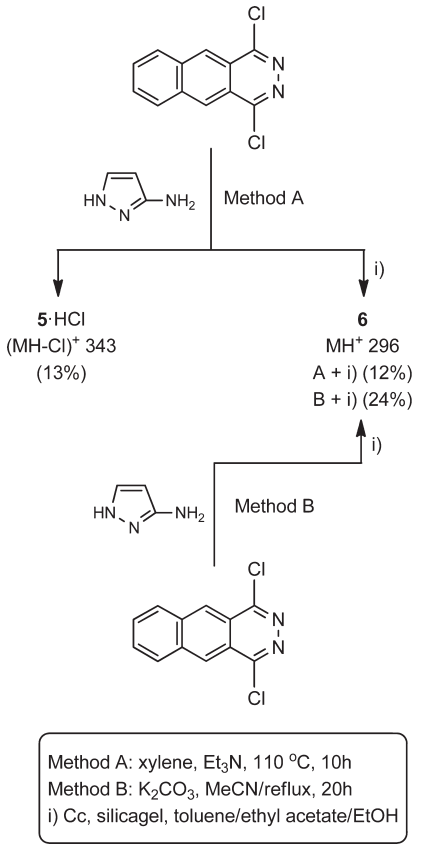

pyridazine and pyrazole nitrogens in metal complexation and modify Fe-SOD inhibition.

In the first part of this study, we describe the synthesis and identification of compounds **5** and **6**, as well as their *in vitro* antiparasitic activity, toxicity, and SOD inhibition indexes in relation to those found previously for compounds **1**−**4** and benznidazole (BZN).[12] Considering the promising *in vitro* results obtained for compounds **1**−**6**, herewith we report a detailed study on the *in vivo* antiparasitic activity and toxicity of these compounds, both in the acute and in the chronic phases. Furthermore, we also include a NMR study concerning the nature and percentage of the excretion metabolites in order to obtain information on the inhibitory effect of our compounds on the glycolytic pathway, since it represents the prime source of energy for the parasite. The effects of compounds **1**−**6** on the ultrastructure of *Trypanosoma cruzi* are also considered on the basis of transmission electronic microscopy (TEM) experiments. Finally, a histopathological analysis is performed in search of better insight into compound toxicity.

## Results and Discussion

**Chemistry.** The preparation of compounds **5** and **6** (Figure 2) was performed from 1,4-dichlorobenzo[*g*]phthalazine as shown in Scheme 1, using similar experimental conditions to those reported by our group for the synthesis of **1**−**4**[12] and other analogs.[11]

Thus, nucleophilic substitution at the C-1 and C-4 positions of the starting compound with 3-aminopyrazole by heating in xylene at 110 °C for 10 h (method A) afforded the bis- and monoalkylamination products **5**·HCl (mp 286 °C) and **6** (mp 235 °C) in 13% and 12% yield, respectively.

Isolation of the disubstituted compound **5**, which was obtained in the hydrochloride form, was straightforwardly achieved by recovering the precipitate (a pure reddish solid). The monosubstituted compound **6** was isolated in the free form from the remaining organic phase after elimination of the solvent under vacuum and purification of the residue by flash chromatography on silica gel with a toluene/ethyl acetate/ethanol mixture of increasing polarity. Alternatively, **6** could be obtained in a higher yield (24%) by refluxing the starting compounds in acetonitrile for 20 h in the presence of potassium carbonate (method B).

Both compounds were unequivocally identified on the basis of their ESI mass spectra, analytical data, and IR, $^1$H NMR, and $^{13}$C NMR spectroscopy. Assignment of the NMR signals could be achieved using bidimensional techniques (gHMQC and gHMBC). The mono- and bis-alkylamination products could be easily differentiated in both $^1$H and $^{13}$C spectra by comparing the $H_5/H_{10}$ and $C_1/C_4$ signals at rings B and A of the benzo[*g*]phthalazine moiety. Disubstituted compound **5**·HCl exhibited a unique signal for $C_1$ and $C_4$ and also for $H_5$ and $H_{10}$ as a singlet. On the contrary, $C_1$ and $C_4$ gave clearly different signals in its monosubstituted analog, being the carbon linked to the chlorine atom shielded about 8 ppm. In a similar way, $H_5$ and $H_{10}$ appeared as two singlets separated by 1.34 ppm, and the proton in the neighborhood of the chlorine was also shielded with respect to the one coplanar with nitrogen. Neat differences were also observed among the hydrogens at ring C in both derivatives, with the disubstituted compound exhibiting the expected symmetrical pattern. It should be noted that the pyrazole NH hydrogens give very low-field signals in the $^1$H NMR spectra (12.2 ppm and 12.7 ppm for **5**·HCl and **6**, respectively). This fact probably indicates the presence of strong N···H···N inter- or intramolecular bonding in both molecules.

Finally, the two ESI mass spectra (positive mode) exhibited molecular ions corresponding to the proposed structures (*m*/*e* 343 $[MH - Cl]^+$ and 296 $[MH^+]$ for **5** and **6**, respectively).

***In Vitro* Anti-*T. cruzi* Activity.** In a first step, the inhibitory effect of the new pyrazole compounds **5** and **6** on the *in vitro* growth of. *T. cruzi* epimastigotes was measured at concentrations ranging from 1 to 100 $\mu$M, and compared with those of the previously synthesized imidazole analogs **1**−**4**.[12] $IC_{50}$ values obtained after 72 h of exposure are shown in Table 1 including benznidazole as the reference drug. The trypanosomicidal activity of the two pyrazole derivatives was similar (monosubstituted **6**, $IC_{50} = 17.5$ $\mu$M) or even slightly higher (disubstituted **5**, $IC_{50} = 32.8$ $\mu$M) than that found for benznidazole (15.8 $\mu$M), although better results were obtained in the case of the imidazole compounds. An evaluation of cytotoxicity using mammalian Vero cells as the cellular model (Table 1) showed that the two pyrazole derivatives were much less toxic than benznidazole and that, as already observed for the imidazole derivatives, the monoalkylamine products were less toxic than the bisalkylamine analogs. On the other hand, the selectivity index calculated for the pyrazole derivatives was about three times (**5**) and nine times (**6**) higher than that of BZN. However, SI values were again significantly lower than those found for the imidazole analogs.

In most activity assays of new compounds against parasites, forms that develop in vectors are used (epimastigotes in the case of *T. cruzi*), because they are easier to handle *in vitro*.

**Table 1.** *In Vitro* Activity, Toxicity and Selectivity Index Found for the Imidazole-Based (**1**−**4**) and Pyrazole-Based (**5**,**6**) Benzo[*g*]phthalazine Derivatives on Epimastigote Forms of *T. cruzi*[a]

| compound | activity $IC_{50}$ ($\mu$M) | toxicity $IC_{50}$[b] ($\mu$M) | SI[d] |
|---|---|---|---|
| benznidazole | 15.83 | 13.56 | 0.85 |
| **1** | 14.2[c] | 88.7[c] | 6.24 |
| **2** | < 0.3[c] | 213.0[c] | 710.0 |
| **3** | < 0.2[c] | 69.3[c] | 346.5 |
| **4** | 13.7[c] | 145.8[c] | 10.64 |
| **5** | 32.8 | 98.3 | 2.99 |
| **6** | 17.5 | 132.6 | 7.58 |

[a] Note: Average of three separate determinations. [b] On Vero cells after 72 h of culture. $IC_{50}$ = the concentration required to give 50% inhibition, calculated by linear regression analysis from the Kc values at concentrations employed (2.5, 25, and 125 $\mu$M for compounds **1**-**4**; 10, 25, and 50 $\mu$M for **5** and **6**). [c] Published in *J. Med. Chem.*[12] [d] Selectivity index = $IC_{50}$ Vero cells/$IC_{50}$ epimastigote.

However, as reported previously for **1**−**4**, we have opted here for including the effect caused by our compounds on the forms that are developed in the host (amastigotes and trypomastigotes), since they are highly informative in determining how the host is really affected.[17]

Figure 3 displays results obtained concerning *T. cruzi* propagation in Vero cells for compounds **5** and **6**. In these assays, we used the $IC_{25}$ of each product as the test dosage, with BZN as the reference drug. When $1 \times 10^5$ Vero cells were incubated for 2 days and then infected with $1 \times 10^6$ metacyclic forms, obtained using methods described in the Experimental Section (control experiment; Figure 3A), the parasites invaded the cells and underwent morphological conversion to amastigotes within 1 day after infection.

On day 10, the rate of host-cell infection reached its maximum. When compound **5** or **6** was added to the infected Vero cells with *T. cruzi* metacyclic forms ($IC_{25}$ concentration), the infection rate significantly decreased with respect to the control, reaching 63% (**5**) and 68% (**6**) on day 10 of the experiment. The decrease in infection rate found for these compounds was substantially higher than the one measured for BZN (39%).

On the other hand (Figure 3B), the average number of amastigotes per infected cell increased to 39.6 amastigotes/cell in the control experiment on day 6, decreasing to a value of 30.6 on day 8 and increasing again to 35.0 on day 10. Those fluctuations in the number of amastigotes could be explained considering that they leave the cell and invade it again in a cyclic way, thus originating new replication and variations in the number of amastigotes per cell. When the pyrazole compounds were tested, both of them inhibited *T. cruzi* amastigote replication in Vero cells. Thus, the addition of a concentration equivalent to the $IC_{25}$ of these compounds produced a remarkable decrease in the amastigote number per infected cell, reaching on day 10 a 56% reduction for **6** and 40% for **5** with respect to the control experiment. These results are striking when compared with those obtained for BZN, which only reached a 15% reduction in the amastigote number.

Rupture of the Vero cell membrane implies liberation of amastigotes and further transformation in trypomastigotes. Therefore, we have also measured the variation in the trypomastigote number in the culture medium (Figure 3C). The control experiment had a trypomastigote number of $4.4 \times 10^4$ on day 10, and reductions of 53% and 63% were found for compounds **5** and **6**, respectively. These reductions were more profound than that obtained for BZN (43%).

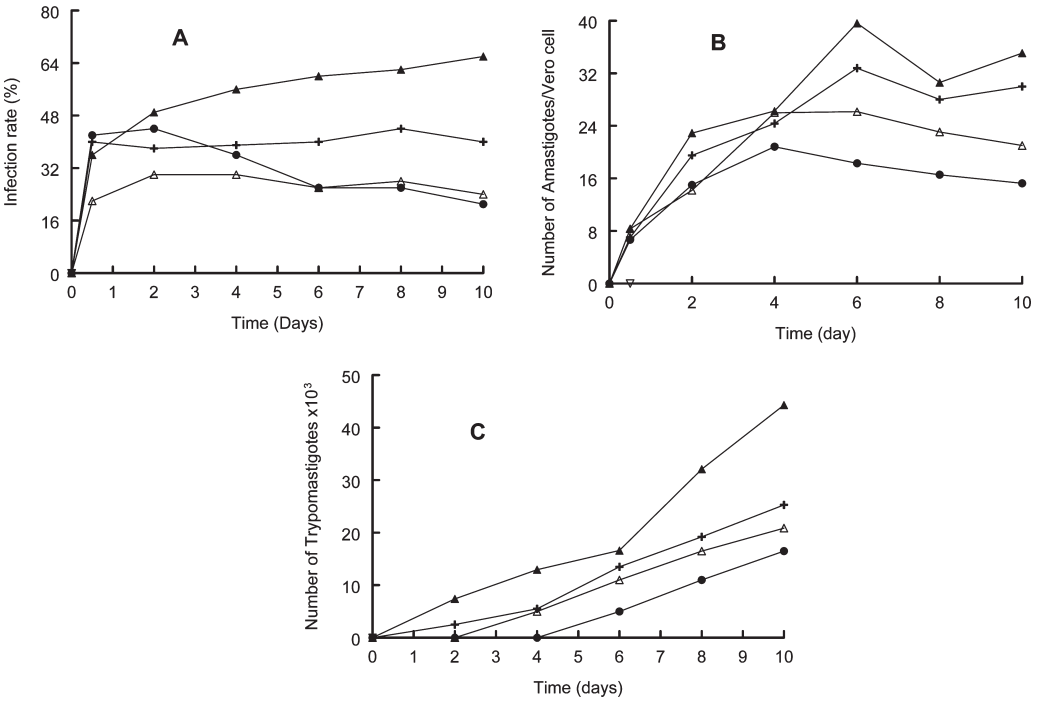


**Figure 3.** Effect of compounds **5** and **6** on the infection rate and *T. cruzi* growth: (A) rate of infection; (B) mean number of amastigotes per infected Vero cell; (C) number of trypomastigotes in the culture medium; (▲) control; (+) BZN; (△) compound **5**; (●) compound **6**. Measured at $IC_{25}$ concentration. Values are means of three separate experiments.

From the data described above and from those reported previously on *T. cruzi* propagation in the presence of **1**−**4** in Vero cells,[12] it can be concluded that the monoalkylamino-substituted compounds **2**, **4**, and **6** are considerably more active than their disubstituted analogs and also that the six compounds tested are more effective than BZN.

***In Vivo* Anti-*T. cruzi* Activity.** The good results obtained in the *in vitro* tests performed on both the imidazole- and pyrazole-based derivatives prompted us to study their *in vivo* activity in mice. We decided to evaluate their impact on the two significant stages of Chagas disease: the acute phase, considered as the first 40 days postinfection, and the chronic phase, from 80 days postinfection. It has been recently published that the intravenous doping route results in high mortality rates,[18] so we opted for the intraperitoneal route, using a concentration of 5 mg/kg, which did not result in any animal mortality. Female Swiss mice were inoculated intraperitoneally with 3000 metacyclic trypomastigotes, and treatment began 7 days postinfection by the ip route with 1 mg/(kg·day) of each compound for 5 days. Administration was performed with a saline solution. A group treated in the same manner with vehicle (control) was included. During the study of the acute phase activity, the level of parasitemia was determined every 2 days (Figure 4A,B). None of the animals treated with either the control or compounds **1**−**6** died during treatment, whereas the survival percentage of the mice treated with BZN was 80%.

A comparison of the data represented in Figure 4A,B showed that, with respect to control mice, the six compounds tested were able to diminish the trypomastigote number on the day of maximum parasitic burden, which was day 25 postinfection. On day 40 pi, a significant reduction of the parasitemia was found for the monoalkylamino-substituted derivatives **2**, **4**, and **6** with respect to the disubstituted derivatives **1**, **3**, and **5**. Additionally, the imidazole-based compound **4** was especially efficient among all the tested compounds. From these data, the following order for *in vivo* activity could be established: **4** > **2** ≈ **6** > **1** ≈ **3** > **5** > BZN.

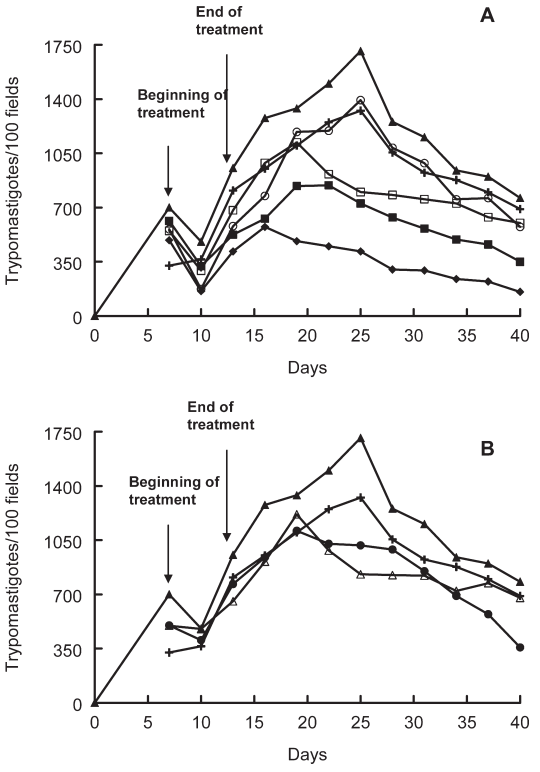


**Figure 4.** Parasitemia in the murine model of acute Chagas disease: (A) control (▲) and receiving 5 mg/kg doses of BZN (+); compound **1** (○); compound **2** (■); compound **3** (□); compound **4** (◆); (B) receiving 5 mg/kg doses of BZN (+); compound **5** (Δ); compound **6** (●).

Concerning the activity in the chronic phase, serological tests were performed 40 and 120 days postinfection (Table 2).

**Table 2.** Differences in the Level of anti-*T. cruzi* Antibodies between Day 40 and Day 120 Post-infection for Compounds **1**−**6** and BZN, Expressed in Absorbance Units (abs)

| compounds[a] | $\Delta A$[b] |
|---|---|
| control (untreated) | 0.146 |
| benznidazole | 0.110 |
| **1** | 0.044 |
| **2** | −0.076 |
| **3** | 0.266 |
| **4** | −0.151 |
| **5** | 0.138 |
| **6** | −0.228 |

[a] Dose of 1 mg/(kg·day), administered by the intraperitoneal route for five days (see Experimental Section). [b] $\Delta A$ = (absorbance at 490 nm on day 120 p.i.) − (absorbance at 490 nm on day 40 p.i.).

None of the animals treated with compounds **1**-**6** or with the control drug BNZ showed negative anti-*T. cruzi* serology. However, the monosubstituted compounds **6**, **4**, and **2** and, to a much lesser extent, the disubstituted analog **1**, decreased antibody levels between days 40 and 120, showing higher performance than BNZ in this assay. Differences in the level of anti-*T. cruzi* antibodies were in agreement with the parasitemia findings.

In summary, it can be concluded that the monoalkylamino-substituted imidazole- or pyrazole-based compounds **4**, **6**, and **2** are remarkably active against *T. cruzi in vitro* and also *in vivo*, both in the acute and in the chronic phase of the infection.

**Studies on the Mechanism of Action.** In order to get some information about the mechanisms of action of compounds **1**−**6** on the parasite, we performed the following experiments:

**(a). Inhibitory Effect on *T. cruzi* Fe-SOD Enzyme.** Previous results concerning the inhibitory activity of compounds **1**−**4** on the essential antioxidant parasite enzyme Fe-SOD[12] prompted us to compare the effect of the whole group of compounds at a range of concentrations from 1 to 100 $\mu$M. We used epimastigote forms from the Maracay strain of *T. cruzi*, which excrete Fe-SOD when cultured in a medium lacking fetal calf serum.[19] Results obtained are displayed in Figure 5A, and the corresponding $IC_{50}$ values have been calculated and included in the same figure. Significant inhibition values of the enzyme activity were found for the six tested compounds, with the monoalkylamino imidazole derivatives **2** and **4** being especially effective at both the lower and higher doses. Compounds **2** and **4** exhibited $IC_{50}$ values of 9.4 and 1.3 $\mu$M, respectively. The activity of the pyrazole-based **6** was lower at a concentration of 50 $\mu$M, with a $IC_{50}$ of 17.2 $\mu$M, although it was more active than the three disubstituted compounds.

In any case, a high degree of activity against the parasitic Fe-SOD would be of no value if the same pattern was found for human SOD. Therefore, we also compared the effect of compounds **1**−**6** over CuZn-SOD from human erythrocytes (Figure 5B). The results show that the degree of inhibition of human CuZn-SOD was very small at both higher and lower doses, with $IC_{50}$ values reaching 103.3, 129.3, and 786.9 $\mu$M for **6**, **4**, and **2**, respectively, in sharp contrast with those calculated in Figure 5A. These results enhance the potential antiparasitic interest of the alkylamino-benzo[*g*]phthalazine derivatives studied in this work and could support a competition for the metal ion of SOD as one of the feasible mechanisms involved.

In order to obtain more information on the higher activity shown by compounds **2** and **4** over Fe-SOD, we performed a

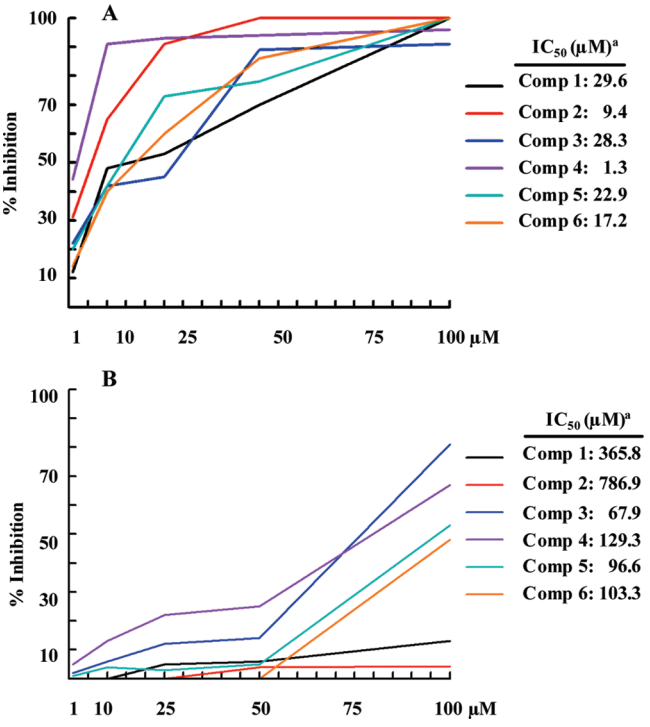


**Figure 5.** (A) *In vitro* inhibition (%) of Fe-SOD in *T. cruzi* epimastigotes for compounds **1**−**6** (activity 20.77 ± 3.18 U/mg). (B) *In vitro* inhibition of CuZn-SOD in human erythrocytes for compounds **1**−**6** (activity 23.36 ± 14.21 U/mg). Values are the average of five separate determinations. Differences between the activities of the control homogenate and those incubated with compounds **1**−**6** were obtained according to the Newman−Keuls test. $IC_{50}$ (the concentration required to give 50% inhibition) was calculated by linear regression analysis from the $K_c$ values at the concentrations employed (1, 10, 25, 50, and 100 $\mu$M).

tentative molecular modeling study on the mode of interaction of the mono- and disubstituted imidazole-based compounds with the enzyme. The *T. cruzi* Fe-SOD structure was obtained from the Brookhaven protein data bank (2gcp). In a first stage, we docked molecules **1**−**4** with the enzyme using the AutoDock 4.2 program.[20] It was found that the preferred location for compounds **2** and **4** was inside the enzyme cavity, although with a poor stabilization energy (1.5 kcal/mol). Interestingly, the disubstituted compounds **1** and **3** were not able to enter the enzyme cavity. The presence of the second alkylamino chain should yield stronger interactions with external amino acids preventing entrance into the cavity. In a further approach, the ability for iron complexation was tested by selecting only one strand of the enzyme and using the AMBER forcefield implemented in Hyperchem 8.0.[21] In all cases, burial of the lateral chain into the protein involved better stabilization energies (15−33 kcal/mol) and considerable shortening of the preferred Fe−N distances to 0.4−0.5 nm.[22] However, a 0.1 nm separation of the two strands was required for allowing compounds **1** and **3** to enter the cavity, and additional destabilization energies of about 40 kcal/mol were found. As shown in Figure 6, the most effective interaction of compound **4** seemed to take place through the $sp^2$ imidazole nitrogens and not with the phthalazine heteroatoms. Although molecular modeling is only an orientative tool, we think that these theoretical results could contribute to explaining the activity differences found between the mono- and disubstituted compounds.

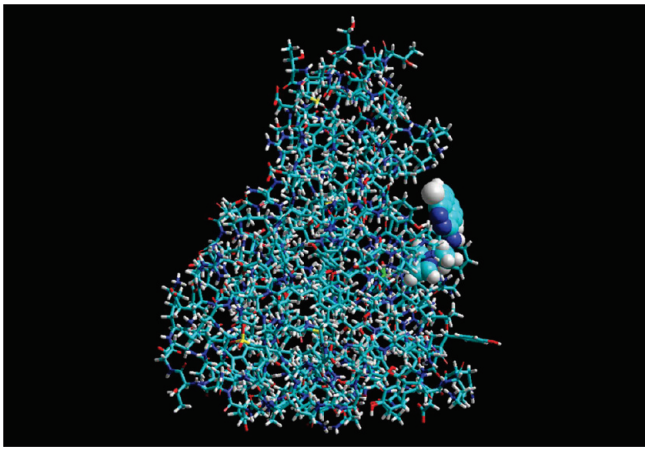

**Figure 6.** Interaction of the imidazole-based monosubstituted compound **4** with one strand of the *T. cruzi* Fe-SOD enzyme (Fe marked in green).

**(b). Metabolite Excretion Effect.** As far as it is currently known, none of the studied trypanosomatids are capable of completely degrading glucose to $CO_2$ under aerobic conditions, and they excrete parts of their carbon skeleton into the medium as fermented metabolites, which differ depending on the species considered.[23] *T. cruzi* consumes glucose at a high rate, thereby acidifying the culture medium due to incomplete oxidation to acids. $^1$H NMR spectra enabled us to determine the fermented metabolites excreted by trypanosomatid in culture. One of the major metabolites excreted by *T. cruzi* is succinate, the main role of which is to probably maintain the glycosomal redox balance. It is thought that succinate provides two glycosomal oxidoreductase enzymes that allow for reoxidation of NADH, produced by glyceraldehyde-3-phosphate dehydrogenase in the glycolytic pathway. Succinic fermentation offers the significant advantage of requiring only half of the phosphoenolpyruvate (PEP) produced to maintain the $NAD^+$/NADH balance. The remaining PEP is converted into acetate, L-lactate, L-alanine, or ethanol, depending on the species considered.

In order to obtain information on the effect of compounds **1**−**6** on metabolite excretion, $^1$H NMR spectra obtained from the trypanosomatids treated with **1**−**4** and **5** and **6** (Figures 1S and 2S, respectively, located in the Supporting Information) were recorded and compared with those obtained from cell-free medium (control) 4 days after inoculation with the *T. cruzi* strain. In the control experiment, *T. cruzi* excreted acetate and succinate as the major metabolites and, at a lower level, L-alanine, in agreement with previously reported data.[24] When trypanosomatids were treated with compounds **1**−**6**, the excretion of some of these catabolites was clearly altered at the dosage employed. The variation in the height of the peaks corresponding to the significant catabolites is shown in Table 3. It can be seen that the excretion of succinate and also of acetate was inhibited by compounds **1**−**4**. The inhibition of acetate and succinate excretion could explain the observed increase in L-alanine production, considering that the imidazole-based compounds operate at the electronic chain level, preventing reducing power recharge, or even that they act on the mitochondria and, consequently, oxidative phosphorylation is affected. The pyrazole-based compounds **5** and **6** exhibited a different behavior. Succinate was the only one of the abovementioned metabolites that was inhibited by compound **5**, and a new peak, which was identified as malate appeared. This could be explained on the basis of its action at the fumarate reductase level, leading to inhibition of succinate formation and excretion of malate. On the other hand, compound **6** could inhibit any of the enzymes involved in the formation of acetate from pyruvate (i.e., succinate dehydrogenase). Both **5** and **6** strongly inhibited lactate excretion, a fact that could be explained by a direct action on the lactic fermentation enzyme. It should be noted that we did not find any significant alteration of fuel metabolism in the presence of benznidazole.

**Table 3.** Variation in the Height of the Peaks Corresponding to Catabolites Excreted by *T. cruzi* Epimastigotes in the Presence of Compounds **1**−**6** with Respect to the Control Test[a]

| compound | Ala | A | S | Lac | Mal |
|---|---|---|---|---|---|
| **1** | +35% | −30% | −39% | = | ud |
| **2** | +22% | −18% | −37% | = | ud |
| **3** | +43% | −22% | −27% | = | ud |
| **4** | +61% | −26% | −49% | = | ud |
| **5** | = | = | −24% | −55% | +100% |
| **6** | = | −36% | +27% | −61% | ud |

[a] Ala, L-alanine; A, acetate; S, succinate; Lac, lactate; Mal, malate; (−) peak inhibition; (+) peak increasing; (=) no difference detected; (ud) peak undetected.

**(c). Ultrastructural Alterations.** We found by transmission electron microscopy (TEM) that morphological alterations are important in *T. cruzi* epimastigotes treated with compounds **1**, **2**, **4**, **5**, and **6** as compared with controls cells (Figure 7). Significant damage was found in the case of compound **1**. Many parasites were dead, and alterations were evident in most of the survivors. Especially significant was the presence of a much higher number of glycosomes than in the control (panel control of Figure 7, panel 1 of Figure 7). An extensive vacuolization was also found in many cases. Vacuolization was also the most characteristic feature observed in parasites treated with compound **2**, together with the presence of cytoplasms containing empty vacuoles and the absence of cytoplasmic organelles (panel 2 of Figure 7).

The most extensive damage was found in parasites treated with compound **4** (panel 4 of Figure 7). The shape of many parasites was so distorted that their morphology was completely unrecognizable, and neither the nucleus not the cytoplasmic organelles could be observed. Many others were dead, and a great number of flagella could be observed inside the supernatant liquid. The few recognizable parasites always presented with empty or lipidic vacuoles. Modifications related to those found with **4** were observed after treatment of the epimastigotes with compound **5** (panel 5 of Figure 7). Most of the cytoplasms were electron dense and exhibited bulk vacuoles, nucleus and shape were also unrecognizable, and both kinetoplasts and mitochondria were inflated. The presence of **6** (panel 6 of Figure 7) also resulted in distorted shapes and strong vacuolization. In summary, a wide range of ultrastructural alterations in epimastigote forms of *T. cruzi* treated with these compounds were found. These alterations, which took place mainly at the mitochondria level, explain the metabolic changes commented above in the production of succinate and acetate and may have been due to disturbances in the activity of enzymes involved in the pyruvate metabolism inside the mitochondria.

**Histopathological Analysis.** In order to get better insight into the toxicity level induced by our compounds on the liver, a key organ in many vital functions, we performed a

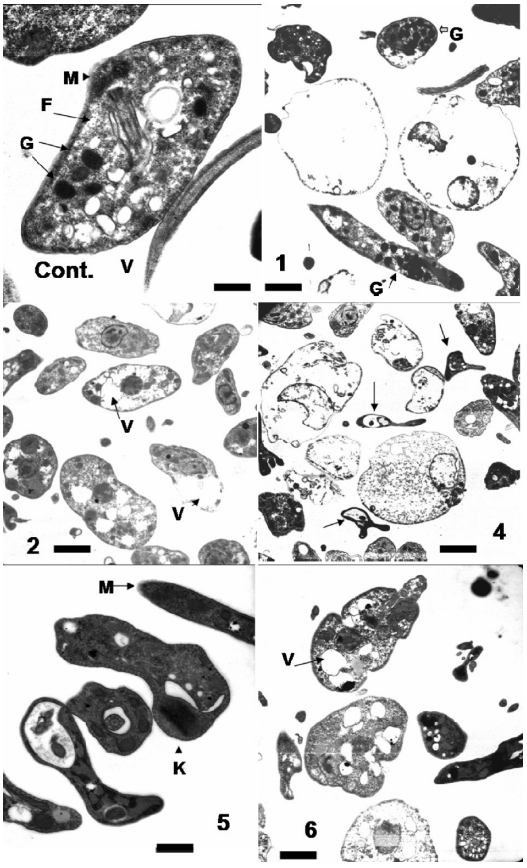


**Figure 7.** Ultrastructural alterations by TEM in *T. cruzi* treated with compounds **1**, **2**, and **4**−**6**: (Cont) control parasite showing organelles with their characteristic aspects, such as nucleus (N), kinetoplast (K), reservosomes (R) mitochondrion (M), flagellum (F), vacuole (V), and glycosomes (G); bar = 583 $\mu$m; (1) epimastigotes of *T. cruzi* treated with compound **1**; bar = 1.00 $\mu$m; (2) epimastigotes of *T. cruzi* treated with compound **2**; bar = 1.59 $\mu$m; (4) epimastigotes of *T. cruzi* treated with compound **4**; bar = 1.59 $\mu$m; (5) epimastigotes of *T. cruzi* treated with compound **5**; bar = 583 $\mu$m; (6) epimastigotes of *T. cruzi* treated with compound **6**; bar = 1.00 $\mu$m.

histopathological analysis on mice infected with the parasite and treated with the monosubstituted compounds **2**, **4**, and **6** (Figure 8). Those compounds were selected because of their especially good activity results in both the *in vivo* and *in vitro* tests. We observed that mice infected but not treated developed several alterations to the liver after 90 days, undoubtedly due to the action of the parasite during the chronic phase. Among them were lymphocytic infiltration with the formation of many microgranulomas (+++++), delocalized hepatic destruction (+++), and, to a lesser extent, lymphocytic infiltration of the portal tracts (++), and interstitial hemorrhage (++). When parasite-infected mice were treated with the reference drug (BZN), lymphocytic infiltration and the formation of granulomas diminished (++), due to the lower number of parasites remaining after drug treatment. In contrast, a significant increase in delocalized hepatic destruction (++++), very severe hepatic destruction in the portal tracts (+++++), and the presence of necrotic cells in those tracts (+++) were found, caused by the toxicity of BZN.

Treatment of infected mice with the monosubstituted compounds also showed some hepatic damage 90 dpi. However, alterations were never as severe as those ones

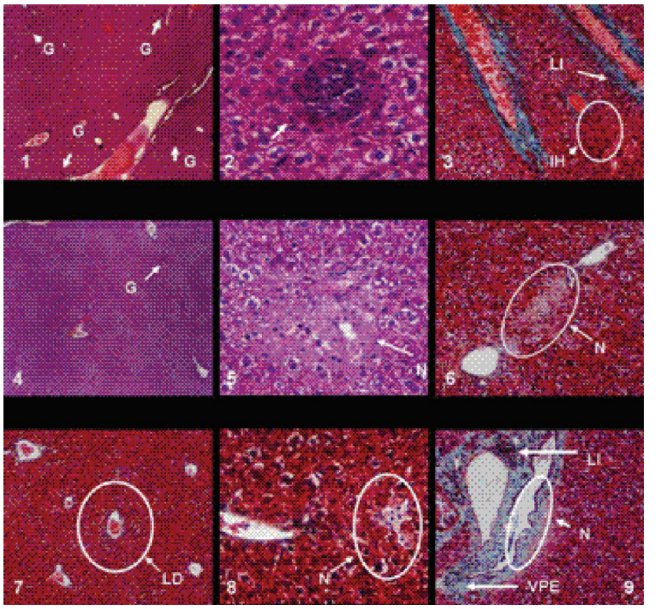


**Figure 8.** Histopathological analysis of the liver. First line: Mice were infected but left untreated for 90 dpi (1) resulting in microgranulomas (G); (2) detail of a microgranuloma; (3) lymphocytic infiltration (LI) and interstitial hemorrhage (IH). Second line shows mice infected and treated with BZN (5 mg/kg) for 90 dpi resulting in (4) microgranulomas (G) and (5, 6) necrosis (N). Third line shows mice infected and treated with the monosubstituted compounds (5 mg/kg) after 90 dpi: (7) compound **2** shows damage in the portal tract zone (LD); (8) compound **4** shows necrosis (N); (9) compound **6** shows lymphocytic infiltration in the portal tract zone (LI), necrosis (G), and thickening of the blood vessel walls in the portal tracts (VPE).

commented on above for BZN, indicating a lower toxicity for the three compounds tested. Only a very slight formation of granulomas with lymphocytic infiltration (+) and minor delocalized hepatic destruction (+) could be detected after treatment with **2**. In the case of **4**, a light thickening of the blood vessel walls was also observed. Pyrazole-based **6** appeared to be a little more toxic, since the livers presented some lymphocytic infiltration in the portal tracts (++), together with a small interstitial hemorrhage (++). We can conclude that, on the hepatic level, our monosubstituted compounds **2**, **4**, and **6** are much less toxic for the host than BZN, and compound **4** is apparently the most benign among the three of them.

## Experimental Section

**Chemistry.** 3-Aminopyrazole was purchased from a commercial source (Aldrich) and used without further purification. 1,4-Dichlorobenzo[*g*]-phthalazine was obtained from 2,3-naphthalenedicarboxylic acid according to a procedure previously reported by our group.[25] Solvents were dried using standard techniques.[26] All reactions were monitored using thin layer chromatography (TLC) on precoated aluminum sheets of silicagel $60F_{254}$. Compounds were detected with UV light (254 nm). Chromatographic separations were performed on columns in the indicated solvent system using flash chromatography on silicagel (particle size 0.040−0.063 mm). Melting points were determined in a Gallenkampf apparatus and were uncorrected. $^1$H NMR spectra were recorded on a Bruker 300 and a Variant XL 300 at 300 MHz and $^{13}$C NMR spectra at 75 MHz at room temperature employing DMSO-$d_6$ as the solvent. Chemical shifts are reported in ppm ($\delta$ scale) from TMS. All assignments were performed on the basis of $^1$H−$^{13}$C heteronuclear multiple

quantum coherence experiments (gHMQC and gHMBC). IR spectra were recorded on a Perkin-Elmer 257 spectrometer (4000−400 $cm^{-1}$ range). Electrospray mass spectra were recorded with a Hewlett-Packard 1100 MSD apparatus. Elemental analyses were performed in a Perkin-Elmer 2400-CHN instrument by the Departamento de Analisis, Centro de Química Orgánica "Manuel Lora-Tamayo", CSIC, Madrid, Spain. Elemental analysis was used to ascertain purity higher than 95% for all the biologically tested compounds.

**Synthesis of 1,4-Bis(3′-pyrazolylamino)benzo[*g*]phthalazine (5) and 4-Chloro-1-(3′-pyrazolylamino)benzo[*g*]phthalazine (6) (Method A).** A solution of 1,4-dichlorobenzo[*g*]phthalazine (278 mg, 1.12 mmol), 3-aminopyrazole (204 mg, 2.45 mmol), and triethylamine (0.6 mL, 3.60 mmol) in xylene (20 mL) was heated at 110 °C for 10 h. After cooling to room temperature, the reaction mixture afforded a reddish precipitate, which was filtered and dried under vacuum, giving 53 mg (13% yield) of a pure crystalline solid that was identified as **5**·HCl. Mp 286 °C (d). IR (KBr) *ν*: 3500−2500, 3137, 2959, 2925, 2855, 1573, 1484, 1440, 1419, 1124, 1048, 999, 924, 894, 748 $cm^{-1}$. $^1$H NMR (DMSO-$d_6$): $\delta$ 12.21 (brsg, 2H, NH pyrazole), 9.49 (s, 2H, H-5, H-10), 8.25 (m, 2H, H-6, H-9), 7.87 (m, 2H, H-7, H-8), 7.79 (d, 2H, H-5′), 6.55 (d, 2H, H-4′). $^{13}$C NMR (DMSO-$d_6$): $\delta$: 149.15 (C-3′), 145.26 (C-1, C-4), 133.99 (C-5a, C-9a), 130.08 (C-5′), 129.45 (C-7, C-8), 128.97 (C-6, C-9), 125.39 (C-5, C-10), 119.54 (C-4a, C-10a), 97.20 (C-4′) ppm. ESI-MS (positive mode, MeOH) *m*/*z* (%): 343 ([MH − Cl]$^+$, 100). Anal. ($C_{18}H_{14}N_8$·HCl·0.5$H_2O$) C, H, N, Cl.

The remaining xylene solution was evaporated under vacuum, and the residue was chromatographed on a silicagel supported column using a mixture of increasing polarity of toluene/ethyl acetate/ethanol as the eluent. From the fraction with $R_f$ = 0.58 (toluene/ethyl acetate/ethanol, v/v = 2:1:0.3), 39 mg (12%) of a yellow solid was isolated and identified as corresponding to the free monosubstituted compound **6**. Mp: 235 °C (desc.). IR (KBr) *ν*: 3000−3500, 3330, 3214, 2923, 2854, 1616, 1566, 1439, 1393, 976, 892, 752 $cm^{-1}$. $^1$H NMR (DMSO-$d_6$): $\delta$ 12.7 (brsg, 1H, NH pyrazole), 10.40 (s, 1H, H-10), 9.01 (s, 1H, H-5), 8.48 (d, 1H, H-5′), 8.43 (m, 1H, H-9), 8.27 (m, 1H, H-6), 7.84 (m, 2H, H-7, H-8), 6.02 (d, 1H, H-4′) ppm. $^{13}$C NMR (DMSO-$d_6$): $\delta$ 159.54 (C-1), 151.69 (C-4), 150.01 (C-3′), 134.44 (C-5a, C-9a), 131.95 (C-5′), 129.66 (C-10), 129.56, 129.47, 129.36, 129.18 (C-6, C-7, C-8, C-9), 125.45 (C-5), 123.31 (C-10a), 118.06 (C-4a), 98.83 (C-4′) ppm. ESI-MS (positive mode, MeOH) *m*/*z* (%): 296 (MH$^+$, 100). Anal. ($C_{15}H_{10}N_5Cl$·0.5$C_2H_5OH$) C, H, N, Cl.

**Alternative Synthesis of 4-Chloro-1-(3′-pyrazolylamino)benzo-[*g*]phthalazine (6) (Method B).** To a suspension, heated at reflux, of 1,4-dichlororobenzo[*g*]phthalazine (450 mg, 1.80 mmol) and potassium carbonate (2.45 g, 17.75 mmol) in acetonitrile (80 mL), 300 mg (3.61 mmol) of 3-aminopyrazole in 30 mL of acetonitrile was added dropwise, and the mixture was heated under reflux for 20 h. After cooling to room temperature, the orange solid containing the reaction product and potassium carbonate was filtered, dissolved in chloroform, and treated with a 20% NaOH aqueous solution. After the organic layer was washed with water and the solvent was evaporated under vacuum, the residue was chromatographed on a silicagel supported column using a mixture of increasing polarity of toluene/ethyl acetate/ethanol as the eluent. From the fraction with $R_f$ = 0.58 (toluene/ethyl acetate/ethanol, v/v=2:1:0.3), 124 mg (24%) of a yellow solid was isolated and identified as indicated above as the free monosubstituted compound **6**.

**Parasite Strain and Culture.** The Maracay strain of *T. cruzi* was isolated at the Institute of Malariology and Environmental Health in Maracay (Venezuela). Epimastigote forms were obtained in biphasic blood-agar NNN medium (Novy−Nicolle−McNeal) supplemented with minimal essential medium (MEM) and 20% inactivated fetal bovine serum and afterward reseeded in a monophasic culture (MTL), following the method of Luque et al.[27]

***In Vitro* Trypanosomicidal Activity Assay.** To obtain the parasite suspension for the trypanosomicidal assay, the epimastigote culture (in the exponential growth phase) was concentrated by centrifugation at 1000*g* for 10 min, and the number of flagellates were counted in a hemocytometric chamber and distributed into aliquots of 2 × $10^6$ parasites/mL. The compounds were solved in DMSO (Panreac, Barcelona, Spain) at a concentration of 0.01%, previously assayed as nontoxic and without inhibitory effects on parasite growth. The compounds were dissolved in the culture medium, and the doses used were 100, 50, 25, 10, and 1 $\mu$M. The effect of each compound against epimastigote forms, as well as the concentrations (assayed at different concentrations for every drug), were evaluated at 72 h, using a Neubauer hemocytometric chamber.

**Cell Culture and Cytotoxicity Tests.** Vero cells (Flow) were grown in MEM (Gibco), supplemented with l0% inactivated fetal calf serum and adjusted to pH 7.2, in a humidified 95% air−5% $CO_2$ atmosphere at 37 °C for 2 days. For the cytotoxicity test, cells were placed in 25 mL colie-based bottles (Sterling) and centrifuged at 100*g* for 5 min. The culture medium was removed, and fresh medium was added to a final concentration of 1 × $10^5$ cells/mL. This cell suspension was distributed in a culture tray (with 24 wells) with 100 $\mu$L/well and incubated for 2 days at 37 °C in a humid atmosphere enriched with 5% $CO_2$. The medium was removed, and fresh medium was added together with the product to be studied (at concentrations of 100, 50, 25, 10 and 1 $\mu$M). The cultures were incubated for 72 h. The vital stain trypan blue (0.1% in phosphate buffer) was used to determine cell viability. The number of dead cells was recorded, and the percent viability was calculated in comparison to that of the control culture. The $IC_{50}$ values were calculated by linear regression analysis from the $K_c$ values at the concentrations employed.

**Transformation of Epimastigotes to Metacyclic Forms.** In order to induce metacyclogenesis, parasites were cultured at 28 °C in modified Grace's medium (Gibco) for 12 days as previously described.[28] Twelve days after cultivation at 28 °C, metacyclic forms were counted in order to infect Vero cells. The proportion of metacyclic forms was around 40% at this stage.

**Cell ®assay.** Vero cells were cultured in MEM medium in a humidified 95% air−5% $CO_2$ atm at 37 °C. Cells were seeded at a density of 1 × $10^5$ cells/well in 24-well microplates (Nunc) with rounded coverslips on the bottom and cultivated for 2 days. Afterward, the cells were infected *in vitro* with metacyclic forms of *T. cruzi*, at a ratio of 10:1. The drugs ($IC_{25}$ concentrations) were added immediately after infection and were incubated for 6 h at 37 °C in a 5% $CO_2$. The nonphagocytosed parasites and drugs were removed by washing, and then the infected cultures were grown for 10 days in fresh medium. Fresh culture medium was added every 48 h.

The drug activity was determined from the percentage of infected cells and the number of amastigotes per cell infected in treated and untreated cultures in methanol-fixed and Giemsa-stained preparations. The percentage of infected cells and the mean number of amastigotes per infected cell were determined by analyzing more than 100 host cells distributed in randomly chosen microscopic fields. Values are the means of four separate determinations. The number of trypomastigotes in the medium was determined as previously described.[28]

***In Vivo* Trypanocidal Activity Assay.** Groups of five BALB/c female mice (6−8 weeks old; 25−30 g) maintained under standard conditions were infected with 3 × $10^3$ bloodstream *T. cruzi* metacyclic forms by the intraperitoneal route. The animals were divided into the following groups: (i) group 1 uninfected (not infected and not treated); (ii) group 2 untreated (infected with *T. cruzi* but not treated); (iii) group 3 uninfected (not infected and treated with 1 mg/kg of body weight/day, for five consecutive days (7−12 days postinfection) by the intraperitoneal route);[18] and (iv) group 4 treated (infected and treated for five consecutive days (7−12 days postinfection) with the compounds and benznidazole).

Five days after infection, the presence of circulating parasites was confirmed by the microhematocrit method. Five microliters of blood drawn from the tail of the treated mice were taken and diluted 1:15 (50 $\mu$L of citrate buffer and 20 $\mu$L of lysis buffer at pH 7.2), and this vehicle also was employed as a negative control. The counting of parasites was done in a Neubauer chamber. The number of deaths was recorded every two days.

One group of four animals treated with each compound and BZN was included for serologic studies. Treatments were started seven days after animal infection. Compounds were administered in a similar way to the methods described above and at the same concentration.

Quantitative evaluation of circulating anti-*Trypanosoma cruzi* antibodies at days 40 and 120 postinfection was carried out by the use of an enzyme-linked immunoassay. The sera, diluted to 1:100, were reacted with an antigen constituted by a soluble Fe-SOD of *T. cruzi* epimastigotes. The results are expressed as the ratio of the absorbance (Abs) of each serum sample at 490 nm to the cutoff value. The cutoff for each reaction was the mean of the values determined for the negative controls plus three times the standard deviation.

**SOD Enzymatic Inhibition in the Presence of Compounds 1−6.** The parasites were cultured as described above and suspended (0.5−0.6 g/mL) in 3 mL of buffer 1 (0.25 M sucrose, 25 mM Tris−HCl, 1 M EDTA, pH 7.8) and disrupted by three cycles of sonic disintegration, 30 s each at 60 V. The sonicated homogenate was centrifuged at 1500*g* for 10 min at 4 °C, and the pellet was washed three times with ice-cold STE buffer 1, for a total supernatant fraction of 9 mL. This fraction was centrifuged (2500*g* for 10 min at 4 °C), the supernatant was collected, and solid ammonium sulfate was added. The protein fraction, which precipitated between 35% and 85% salt concentration, was centrifuged (9000*g* for 20 min at 4 °C), redissolved in 2.5 mL of 20 mM potassium phosphate buffer (pH 7.8) containing 1 mM EDTA (buffer 2), and dialyzed in a Sephadex G-25 column (Pharmacia, PD 10), previously balanced with buffer 2, bringing it to a final volume of 3.5 mL (fraction of the homogenate). The protein concentrations were determined by the Bradford method.

Iron superoxide dismutase (Fe−SOD) activity was determined by NAD(P)H oxidation according to Paoletti and Mocali.[29] One unit was the amount of enzyme required to inhibit the rate of NAD(P)H reduction by 50%. CuZn-SOD from human erythrocytes used in these assays was obtained from Boehringer (Mannheim), while all the coenzymes and substrates came from Sigma Chemical Co. Data obtained were analyzed according to the Newman−Keuls test.

**Metabolite Excretion.** Cultures of *T. cruzi* epimastigotes (initial concentration $5 \times 10^5$ cells/mL) received $IC_{25}$ of the compounds (except for control cultures). After incubation for 72 h at 28 °C, the cells were centrifuged at 400*g* for l0 min. The supernatants were collected to determine excreted metabolites by nuclear magnetic resonance spectroscopy ($^1$H NMR) as previously described by Fernández-Becerra et al.[30] Chemical shifts were expressed in parts per million (ppm), using sodium 2,2-dimethyl-2-silapentane-5-sulfonate as the reference signal and were used to identify the respective metabolites, resulting in findings consistent with those described by Fernández-Becerra et al.[30]

**Ultrastructural Alterations.** The parasites, at a density of $5 \times 10^6$ cells/mL, were cultured in their corresponding medium, containing the drugs at the $IC_{25}$ concentration. After 72 h, the cultures were centrifuged at 400*g* for 10 min, and the pellets were washed in PBS and then fixed with 2% (v/v) formaldehyde−glutaraldehyde in 0.05 M cacodylate buffer (pH 7.4) for 2 h at 4 °C. Pellets were prepared for transmission electron microscopy following the technique of Luque et al.[27]

**Histopathological Analysis.** At 90 dpi, livers were removed, cut longitudinally, rinsed in ice-cold PBS, and fixed in 10% buffered formalin. The tissues were dehydrated and embedded in paraffin. Sections were cut at a thickness of 4−5 $\mu$m and stained with Giemsa, hematoxylin−eosin, and Masson's trichrome. Slides were coded for blinded analysis and histological examinations were performed using a conventional light microscope and were visualized in at least 30 fields (total magnifications, ×40, ×100, ×200, and ×400) for each slide. Histological alterations were given a score of 0 (−) to 5 (+++++), with 0 representing the complete absence of alterations and 5 representing the most severe alterations, respectively.

**Acknowledgment.** The authors thank the Santander-Universidad Complutense Research Program (Grant GR58/08-921371-891), the Spanish MEC Project (Grant CGL2008-03687-E/BOS), and the MCINN Projects (CTQ2009-14288-C04-01 and Consolider CSD2010-00065) for financial support. We are also grateful to the NMR and Microanalysis C.A.I.s of the Universidad Complutense and the Departamento de Analisis del Centro Nacional de Quimica Organica Manuel Lora-Tamayo (C.S.I.C) and also to the transmission electron microscopy and nuclear magnetic resonance spectroscopy services of the CIC-University of Granada.

**Supporting Information Available:** Details on combustion analysis and the NMR spectra obtained from the metabolite excretion studies. This material is available free of charge via the Internet at http://pubs.acs.org.

## References

(1) Souza, W. Chagas' disease: Facts and reality. *Microbes Infect.* **2007**, *9*, 544–545.
(2) Maya, J. D.; Cassels, B. K.; Iturriaga-Vasques, P.; Ferreira, J.; Faundez, M.; Galanti, N.; Ferreira, A.; Morello, A. Mode of action of natural and synthetic drugs against *Trypanosoma cruzi* and their interaction with the mammalian host. *Comp. Biochem. Physiol., Part A* **2007**, *146*, 601–620.
(3) Brener, Z.; Gazzinelli, R. T. Inmunological control of *Trypanosoma cruzi* infection and pathogenesis of Chagas' disease. *Int. Arch. Allergy Inmunol.* **1997**, *114*, 103–110.
(4) http:/www.who.int/whr/2001/en/annex2_en.pdf.
(5) Croft, S.; Barrett, M.; Urbina, J. Chemotherapy of trypanosomiases and leishmaniasis. *Trends Parasitol.* **2005**, *21*, 508–512.
(6) Hinojosa-Valdez, R.; Düsman-Tonin, L. T.; Ueda-Nakamura, T.; Dias-Filho, B. P.; Morgado-Diaz, A.; Sarragiotto, M. H.; Vataru-Nakamura, C. Biological activity of 1,2,3,4-tetrahydro-$\beta$-carboline-3-carboxamides against *Trypanosoma cruzi*. *Acta Trop.* **2009**, *110*, 7–14.
(7) Charmantray, Roldos, V.; Nakayama, H.; Rolon, M.; Montero-Torres, A.; Trucco, F.; Torres, S.; Vega, C.; Marrero-Ponce, Y.; Heguaburu, V.; Yaluff, G.; Gomez-Barrio, A.; Sanabria, L.; Ferreira, M. E.; Rojas de Arias, A.; Pandolfi, E. Activity of a hydroxibibenzyl bryophite constituent against *Leishmania spp* and *Trypanosoma cruzi*: In silico, in vitro, and in vivo activity studies. *Eur. J. Med. Chem.* **2008**, *43*, 1797–1807.
(8) Barrett, M. P.; Gilbert, I. H. F Perspectives for new drugs against Trypanosomiasis and Leishmaniasis. *Curr. Top. Med. Chem.* **2002**, *2* (5), 471–482.
(9) (a) Mehlotra, R. K. Antioxidant defense mechanisms in parasitic protozoa. *Crit. Rev. Microbiol.* **1996**, *22* (4), 295–314. (b) Atwood, J. A., 3rd; Weatherly, D. B.; Minning, T. A.; Bundy, B.; Cavola, C.; Opperdoes, F. R.; Orlando, R.; Tarleton, R. L. The *Trypanosoma cruzi* proteome. *Science* **2005**, *309*, 473–476.
(10) Heby, O.; Persson, L.; Rentala, M. Targeting the polyamine biosynthetic enzymes: A promising approach to therapy of African sleeping sickness, Chagas Disease, and Leishmaniasis. *Amino Acids* **2007**, *33*, 259–266.
(11) Rodriguez-Ciria, M.; Sanz, A. M.; Yunta, M. J. R.; Gomez-Contreras, F.; Navarro, P.; Sanchez −Moreno, M.; Boutaleb-Charki, S.; Osuna, A.; Castiñeiras, A.; Pardo, M.; Cano, C.; Campayo, L. 1,4-Bis(alkyl-amino)benzo[g]phthalazines able to form complexes of Cu(II) which as free ligands behave as SOD inhibitors and show efficient in vitro activity against *Trypanosoma cruzi*. *Bioorg. Med. Chem.* **2007**, *15*, 2081–2091.
(12) Sanz, A. M.; Gomez-Contreras, F.; Navarro, P.; Sánchez-Moreno, M.; Boutaleb-Charki, S.; Campuzano, J.; Pardo, M.; Osuna, A.; Cano, C.; Yunta, M. J. R.; Campayo, L. Efficient inhibition of Fe-SOD

and of *Trypanosoma cruzi* growth by benzo[*g*]phthalazine derivatives functionalized with one or two imidazole rings. *J. Med. Chem.* **2008**, *51* (6), 1962–1966.
(13) Johnson, F.; Giulivi, C. Superoxide dismutases and their impact upon human health. *Mol. Aspects Med.* **2005**, *26*, 340–352.
(14) Elguero, J.; Goya, P.; Jagerovic, N.; Silva, A. M. S. Pyrazoles as drugs: Facts and fantasies. In *Targets in Heterocyclic Systems*; Attanasi, O. A., Spinelli, D., Eds.; The Royal Society of Chemistry: Cambridge, U.K., 2002; Vol. 6, pp 52−98.
(15) Kleingele, J.; Dechart, S.; Meyer, F. Polynuclear transition metal complexes of metal···metal-bridging compartmental pyrazolate ligands. *Coord. Chem. Rev.* **2009**, *253*, 2698–2741.
(16) Perez., J.; Riera., L. Pyrazole complexes and supramolecular chemistry. *Eur. J. Inorg. Chem.* **2009**, 4913–4925.
(17) Boutaleb-Charki, S.; Marín, C.; Maldonado, C. R.; Rosales, M. J.; Urbano, J.; Gutierrez-Sánchez, R.; Quiros, M.; Salas, J. M.; Sánchez-Moreno, M. Copper (II) complexes of [1,2,4]triazolo [1,5-a]pyrimidine derivatives as potential anti-parasitic agents. *Drug Metab. Lett.* **2009**, *3*, 35–44.
(18) Da Silva, C. F.; Batista, M. M.; Batista, D. G. J.; de Souza, E. M.; da Silva, P. B.; de Oliveira, G. M.; Meuser, A. S.; Shareef, A. R.; Boykin, D. W.; Soeiro, M. N. C. In vitro and in vivo studies of the trypanocidal activity of a diarylthiophene diamidine against *Trypanosoma cruzi*. *Antimicrob. Agents Chemother.* **2008**, *9*, 3307 3314.
(19) Villagran, M. E.; Marin, C.; Rodriguez-González, I.; de Diego, J. A.; Sanchez-Moreno, M. Use of an iron superoxide dismutase excreted by *T. cruzi* in the diagnosis of Chagas disease: Seroprevalence in rural zones of the state of Queretaro, Mexico. *Am. J. Trop. Med. Hyg.* **2005**, *73*, 510–516.
(20) Morris, G. M.; Huey, R.; Lindstrom, W.; Sanner, M. F.; Belew, R. K.; Goodsell, D. S.; Olson, A. J. Autodock 4 and autodock tools 4: automated dockingwith selective receptor flexibility. *J. Comput. Chem.* **2009**, *30*, 2785.
(21) HyperChem(TM) Professional 8.0, Hypercube, Inc., 1115 NW 4th Street, Gainesville, Florida 32601, USA
(22) Starting structures for compounds **1**−**4** were built by using Hyperchem capabilities. Its geometry was minimized to a maximum energy gradient of 0.1 kcal/(A mol) with the AMBER force field, using the Polak-Ribiere (conjugate gradient) minimizer, and a "simulated annealing" procedure was used to cover all conformational space. This geometry was always used in all calculations of host/guest complexes. To mimic the conditions used in the factivity measurements, that is, water as solvent, all calculations were carried out *in vacuo* with a distance-dependent dielectric value.
(23) (a) Bringaud, F.; Riviere, L.; Coustou, V. Energy metabolism of Trypanosomatids: Adaptation to available carbon sources. *Mol. Biochem. Parasitol.* **2006**, *149* (1), 1–9. (b) Ginger, M. Trypanosomatid biology and euglenozoan evolution: New insights and shifting paradigms revealed through genome sequencing. *Protist* **2005**, *156* (4), 377–292.
(24) Turrens, J. More differences in energy metabolism between Trypanosomatidae. *Parasitol. Today* **1999**, *15* (8), 346–348.
(25) Campayo, L.; Navarro, P. Synthesis and cytostatic activity of 1,4-bis(alkylamino)-benzo[g]phthalazines with complexing properties. *Eur. J. Med. Chem.* **1986**, *21*, 143–149.
(26) Perrin, D. D.; Armarego, W. L. F.; Perrin, D. R. *Purification of Laboratory Chemicals*; Pergamon Press: Oxford, 1980.
(27) Luque, F.; Fernández-Ramos, C.; Entrala, E.; Rosales, M. J.; Navarro, J. A.; Romero, M. A.; Salas-Peregrín, J. M.; Sánchez-Moreno, M. In vitro evaluation of newly synthesised [1,2,-4]triazolo[1,5-a] pyrimidine derivatives against *Trypanosoma cruzi*, *Leishmania donovani* and *Phytomonas staheli*. *Comp. Biochem. Physiol.* **2000**, *126* (1), 39–44.
(28) Osuna, A.; Adroher, F. J.; Lupiañez., J. A. Influence of electrolytes and non-electrolytes on growth and differentiation of *Trypanosoma cruzi*. *Cell Differ. Dev.* **1990**, *30* (2), 89–95.
(29) Paoletti, F.; Mocali, A. Determination of superoxide dismutase activity by purely chemical system based on NAD(P)H oxidation. *Methods Enzymol.* **1990**, *186*, 209–220.
(30) Fernandez-Becerra, C.; Sánchez-Moreno, M.; Osuna, A.; Opperdoes, F. R. Comparative aspects of energy metabolism in plant trypanosomatids. *J. Eukaryotic Microbiol.* **1997**, *44* (5), 523–529.